

## **Wetting transitions on superhydrophobic auxetic metamaterials**

ARMSTRONG, Steven <<http://orcid.org/0000-0002-0520-8498>>, MCHALE, Glen <<http://orcid.org/0000-0002-8519-7986>>, ALDERSON, Andrew <<http://orcid.org/0000-0002-6281-2624>>, MANDHANI, Shruti <<http://orcid.org/0000-0001-7458-3980>>, MEYARI, Mahya <<http://orcid.org/0009-0001-6371-4997>>, WELLS, Gary G <<http://orcid.org/0000-0002-8448-537X>>, CARTER, Emma <<http://orcid.org/0000-0002-0011-9605>>, LEDESMA-AGUILAR, Rodrigo <<http://orcid.org/0000-0001-8714-0556>> and SEMPREBON, Ciro <<http://orcid.org/0000-0001-9969-0168>>

Available from Sheffield Hallam University Research Archive (SHURA) at:

<https://shura.shu.ac.uk/32784/>

---

This document is the Published Version [VoR]

### **Citation:**

ARMSTRONG, Steven, MCHALE, Glen, ALDERSON, Andrew, MANDHANI, Shruti, MEYARI, Mahya, WELLS, Gary G, CARTER, Emma, LEDESMA-AGUILAR, Rodrigo and SEMPREBON, Ciro (2023). Wetting transitions on superhydrophobic auxetic metamaterials. *Applied Physics Letters*, 123: 151601. [Article]

---







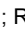


### **Copyright and re-use policy**

See <http://shura.shu.ac.uk/information.html>

RESEARCH ARTICLE | OCTOBER 10 2023

## Wetting transitions on superhydrophobic auxetic metamaterials

Special Collection: [Superhydrophobic Surfaces](#)

Steven Armstrong ; Glen McHale ; Andrew Alderson ; Shruti Mandhani ; Mahya Meyari ; Gary G. Wells ; Emma Carter ; Rodrigo Ledesma-Aguilar ; Ciro Semperebon 



*Appl. Phys. Lett.* 123, 151601 (2023)

<https://doi.org/10.1063/5.0173464>



View  
Online



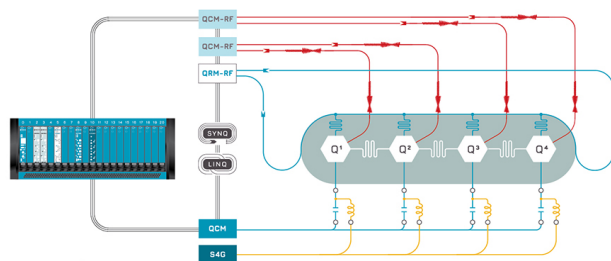
Export  
Citation

CrossMark



Integrates all  
Instrumentation + Software  
for Control and Readout of

**Superconducting Qubits**  
**NV-Centers**  
**Spin Qubits**



Superconducting Qubit Setup

[find out more >](#)

# Wetting transitions on superhydrophobic auxetic metamaterials

Cite as: Appl. Phys. Lett. **123**, 151601 (2023); doi: [10.1063/5.0173464](https://doi.org/10.1063/5.0173464)

Submitted: 22 August 2023 · Accepted: 24 September 2023 ·

Published Online: 10 October 2023



View Online



Export Citation



CrossMark

Steven Armstrong,<sup>1,a)</sup> Glen McHale,<sup>1,a)</sup> Andrew Alderson,<sup>2</sup> Shruti Mandhani,<sup>2</sup> Mahya Meyari,<sup>1</sup> Gary C. Wells,<sup>1</sup> Emma Carter,<sup>2</sup> Rodrigo Ledesma-Aguilar,<sup>1</sup> and Ciro Semprebón<sup>3</sup>

## AFFILIATIONS

<sup>1</sup>Wetting, Interfacial Science and Engineering Laboratory, Institute for Multiscale Thermofluids, The University of Edinburgh, Edinburgh, United Kingdom

<sup>2</sup>Materials and Engineering Research Institute, Sheffield Hallam University, Sheffield, United Kingdom

<sup>3</sup>Smart Materials and Surfaces Laboratory, Faculty of Engineering and Environment, Northumbria University, Newcastle upon Tyne, NE1 8ST, United Kingdom

**Note:** This paper is part of the APL Special Collection on Superhydrophobic Surfaces.

<sup>a)</sup>Authors to whom correspondence should be addressed: [steven.armstrong@ed.ac.uk](mailto:steven.armstrong@ed.ac.uk) and [glen.mchale@ed.ac.uk](mailto:glen.mchale@ed.ac.uk)

## ABSTRACT

Superhydrophobicity plays a pivotal role in numerous applications. Recently, we have demonstrated the potential of auxetic metamaterials in creating superhydrophobic materials with unique wetting properties. However, the superhydrophobic properties are lost when the liquid penetrates into the surface structure. Understanding the conditions for droplet penetration is crucial for advancing wetting control. Here, we experimentally identify the transition from droplet suspension to full-penetration on an auxetic bowtie/honeycomb lattice membrane. We develop a comprehensive physical model surface representing different states of strain, ranging from auxetic to conventional lattice membranes, and consider the wetting as the liquid surface tension is varied using water/ethanol mixtures. By examining the interplay between contact angle and lattice structure, we gain valuable insights into the conditions for droplet suspension and full-penetration. Additionally, we develop a simple touch test to discern whether a droplet has effectively fully penetrated the structure, providing a practical and efficient means of distinguishing the different wetting states (suspended or partially penetrating vs fully penetrating).

© 2023 Author(s). All article content, except where otherwise noted, is licensed under a Creative Commons Attribution (CC BY) license (<http://creativecommons.org/licenses/by/4.0/>). <https://doi.org/10.1063/5.0173464>

Superhydrophobicity is a leading strategy in increasing droplet mobility on surfaces by reducing the solid–liquid interfacial area inspired by the lotus effect.<sup>1,2</sup> Reducing the solid–liquid surface area fraction below a droplet can amplify the apparent contact angle a droplet makes with the surface far beyond ca. 120°, which is the limit of what chemistry can achieve alone using hydrophobic chemistries, such as polytetrafluoroethylene (PTFE).<sup>3</sup> In the field of metamaterials, the lattice structure plays a crucial role in determining unique physical properties.<sup>4–6</sup> Specifically, auxetic metamaterials exhibit the counterintuitive behavior of expanding in an orthogonal direction when stretched, creating additional space between their solid components without stretching or compressing those components themselves.<sup>7–9</sup> Recently we have shown auxetic metamaterials that create a monotonic expansion of the space fraction leading to increased superhydrophobicity with increasing tensile strain.<sup>10</sup> This is a paradigm shift in the engineering of superhydrophobic surfaces, where typically a static arrangement of the structure is considered or a

strain-induced change in superhydrophobicity using a conventional material.<sup>1–3,11,12</sup> When a droplet is in contact with a structured surface, it can be considered as in one of three states, suspended, partially penetrated or fully penetrated. For superhydrophobicity, suspension is the ideal state, where a droplet is only in contact with the top surface of the structure, this allows for the intended amplification of the contact angle and allows the droplet to easily roll-off the surface with little force. In a fully penetrated state, a droplet will wick into the structure, increasing the force required to shed the droplet, often causing the droplet to be pinned.<sup>13–17</sup> In principle, a third, partially penetrated state exists, although for vertical walled structures once penetration begins and a contact line advances down the walls, surface energy arguments suggest complete penetration will occur unless some heterogeneity causes pinning; in this work, we regard this possibility as part of the suspended state. Understanding the fully penetrated state into superhydrophobic surfaces is of great importance.

We can exemplify the difference between conventional and auxetic behavior by considering a hexagonal lattice consisting of inextensible solid elements that can rotate about their connecting nodes when subjected to a mechanical force [Fig. 1(a)]. When this lattice is stretched, the rotation of the solid ribs causes the lattice to contract laterally. This corresponds to positive (extensile) and negative (contractile) strains along and perpendicular to the direction of stretch, respectively, and is characteristic of a positive Poisson's ratio ( $\nu$ —defined as the negative ratio of transverse strain to longitudinal strain). Now, consider transforming the hexagonal lattice into a bow-tie lattice by flipping the angles at two opposing nodes from obtuse to acute in each hexagonal unit [Figs. 1(a) and 1(b)]. The bow-tie lattice expands laterally when stretched lengthwise [Fig. 1(b)], corresponding to a negative Poisson's ratio. The sign, and magnitude, of the lattice Poisson's ratio is then determined by the geometry of the lattice.<sup>18</sup> The opening of the bow-tie due to lengthwise stretching shown in Fig. 1(b) is accompanied by a decrease in the magnitude of the negative Poisson's ratio, which reaches zero when the lattice becomes a rectangular lattice (not shown). Further stretching transforms the lattice into a conventional hexagonal lattice with concomitant transition to a positive Poisson's ratio [Fig. 1(a)], which increases in magnitude as the hexagonal cells become longer and narrower.

An increase in the surface area of a material under tension occurs as long as the Poisson's ratio remains less than +1.<sup>10</sup> Importantly, the increase in surface area is due to the expansion of space within the lattice, not the solid elements themselves. Consequently, the solid surface fraction ( $f_s$ ) decreases as the lattice is stretched when  $\nu < +1$  (this includes all bow-tie configurations, the transition of the bow-tie lattice to a hexagonal lattice geometry, and some—but not all—conventional hexagonal lattice configurations upon stretching). Further stretching of the lattice ( $\nu > +1$ ) leads to a decrease in surface area and an increase

in the solid surface fraction. From the perspective of non-wettable materials, an initially hydrophobic bow-tie lattice metamaterial supporting a droplet in a Cassie–Baxter suspended state will become progressively more hydrophobic and eventually superhydrophobic (including a minimum in solid surface fraction following the transition to a positive Poisson's ratio for a hexagonal lattice), before returning to a hydrophobic state with further stretching. Similarly, one can imagine new and unique superhydrophilic wettable, hemiwicking, and liquid-infused auxetic materials.<sup>19,20</sup>

If a droplet is in a suspended state, it sits on the top surface of the membrane and if fully penetrated it wicks into the structure [Fig. 1(c)]. A droplet state whether suspended or fully penetrated is determined by the interplay between the solid fraction,  $f_s$ ; roughness,  $r_w$ ; and the contact angle of the surface chemistry,  $\theta$ . For an auxetic bow tie lattice with fixed rigid ribs, inducing a strain changes the auxetic rotation angle,  $\alpha$  [Fig. 1(d)]. This in turn modifies the solid fraction and roughness. The concentration of ethanol in a water/ethanol droplet can be correlated with a contact angle on a smooth surface with the same surface chemistry as that on the membrane surface. In soil science, this technique is known as the molarity of ethanol (EtOH) droplet (MED) test and is widely used to quantify the severity of water repellency in soils.<sup>21–24</sup> Figure 1(e) is a phase diagram showing whether a droplet with a specific static contact angle on flat surface will be suspended or fully penetrated on the membrane. We can traverse the graph vertically by fixing the auxetic rotation angle and using increasing EtOH concentration to induce a droplet transition from suspension to full-penetration. Alternatively, we can traverse the graph horizontally by fixing the EtOH concentration and changing the auxetic rotation angle to induce droplet suspension for low auxetic rotation angles, full-penetration around the transition from auxetic to conventional, and suspension again for high conventional rotation angles.

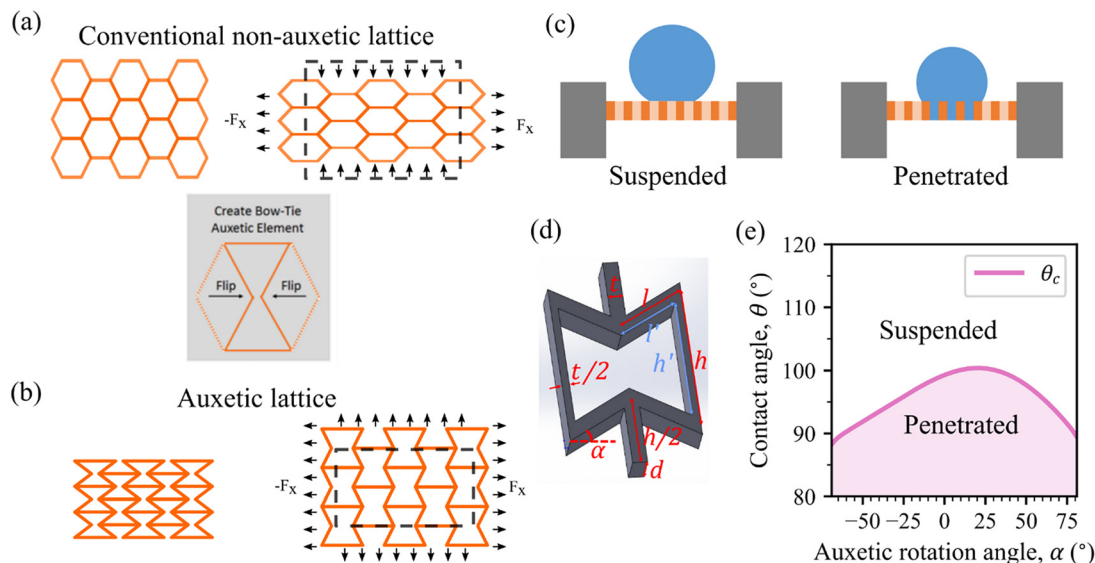


**FIG. 1.** (a) Different strain response of conventional and (b) auxetic honeycomb lattice. (c) Diagram of droplet on a membrane in a suspended state and wicked into a fully penetrated state. (d) Geometric parameters for membrane unit cell. (e) Critical contact angle as a function of auxetic rotation angle for a bowtie auxetic lattice ( $\alpha < 0^\circ$ ), rectangular lattice ( $\alpha = 0^\circ$ ), to conventional honeycomb lattice ( $\alpha > 0^\circ$ ). If the equilibrium contact angle on a solid flat surface is in the shaded region, a fully penetrated state is preferred, else the droplet will be in a suspended state.

We created the model auxetic membranes through a previously developed methodology (supplementary material).<sup>10</sup> We construct a series of model surfaces with fixed auxetic rotation angles from  $-40^\circ$  to  $+70^\circ$ , which enables a direct comparison between the contact angle response and the auxetic rotation angle as opposed to straining a single physical membrane, which would be subject to flexing and stretching of the solid elements. After fabrication, SEM images of representative auxetic and conventional membranes were taken [Figs. 2(a) and 2(b), respectively]. Additionally, an isometric view of a typical auxetic membrane was used to confirm the side walls of the membrane were vertical [Fig. 2(c)]. The SEM images yield average geometrical parameters:  $h = 101.3 \pm 1.1 \mu\text{m}$ ,  $l = 51.5 \pm 2.1 \mu\text{m}$ ,  $t = 18.5 \pm 0.8 \mu\text{m}$ , and  $d = 129.2 \pm 1.2 \mu\text{m}$ . To render the membranes hydrophobic, they were fluorosilanized (supplementary material). To characterize the surface wetting properties, 4.0  $\pm$  0.1  $\mu\text{l}$  water/EtOH mixtures (0%–100% concentration,  $c$ , by volume of EtOH in 10% increments) are placed on the membranes with contact angle measurements and contact angle hysteresis measurements taken on a bespoke goniometry setup, which allows for the suspension of the SU8 lattices (supplementary material).

The auxetic lattices studied here are thin (ca. 130  $\mu\text{m}$ ) suspended membranes and not bulk porous media. Droplets penetrating into membranes do not wick completely through the sample and drip from the bottom of the membrane, but rather liquid fills and is retained in the pores directly underneath the droplet with a droplet remaining visible. Visually, it is, therefore, difficult to determine whether a droplet is suspended or fully penetrated. We identified that a simple touch test to discern whether a droplet has effectively fully penetrated the structure provides a practical and efficient means of distinguishing the different wetting states (suspended vs fully penetrating). If the membrane

suspends the droplet, touching the underside of the membrane will leave the droplet undisturbed. However, if the droplet has fully penetrated the membrane, touching the underside of the membrane will cause the droplet to fully wick through. In our experiments, a flat metal rod held vertically underneath the membrane is gently raised to touch the underside of the lattice. If the droplet is suspended, the liquid will not contact the rod and so will remain unchanged as illustrated in Figs. 2(d) and 2(e) using a water droplet (see also supplementary video SV1.). For 100% EtOH, the droplet initially makes a sessile droplet shape with the surface and, while it has a visibly lower contact angle than the water droplet, it cannot be visually determined whether it has fully penetrated through the lattice [Fig. 2(f)]. However, the penetration test induces the droplet to drain through the membrane and wet the metal rod as illustrated in [Fig. 2(g)] (see also supplementary video SV2.). As the water is suspended and the EtOH is fully penetrated, using mixtures of water/EtOH allows us to control the surface tension and this simple touch test allows the droplet state to be identified. Hence, the critical concentration of EtOH at which the transition from suspension to full-penetration occurs can be identified and this can be correlated with an equivalent contact angle on a smooth surface.

We first look at how the contact angle of the droplet changes with varying EtOH concentration on solid flat fluorosilanized SU8 (Fig. 3). Water has a static contact angle,  $\theta_s(c = 0\%) = 117 \pm 1.7^\circ$ , where the change in contact angle with increasing concentration can be well described using a second-degree polynomial fit (supplementary material), with pure EtOH  $\theta_s(c = 100\%) = 60.1 \pm 1.5^\circ$ . As the contact angle hysteresis of water on flat fluorosilanized SU8 is significant,  $\Delta\theta_{CAH}(c = 0\%) = 35.8^\circ$  with  $\theta_A(c = 0\%) = 120.3 \pm 0.6^\circ$  and  $\theta_R(c = 0\%) = 84.5 \pm 4.6^\circ$ , additional measurements of contact angle

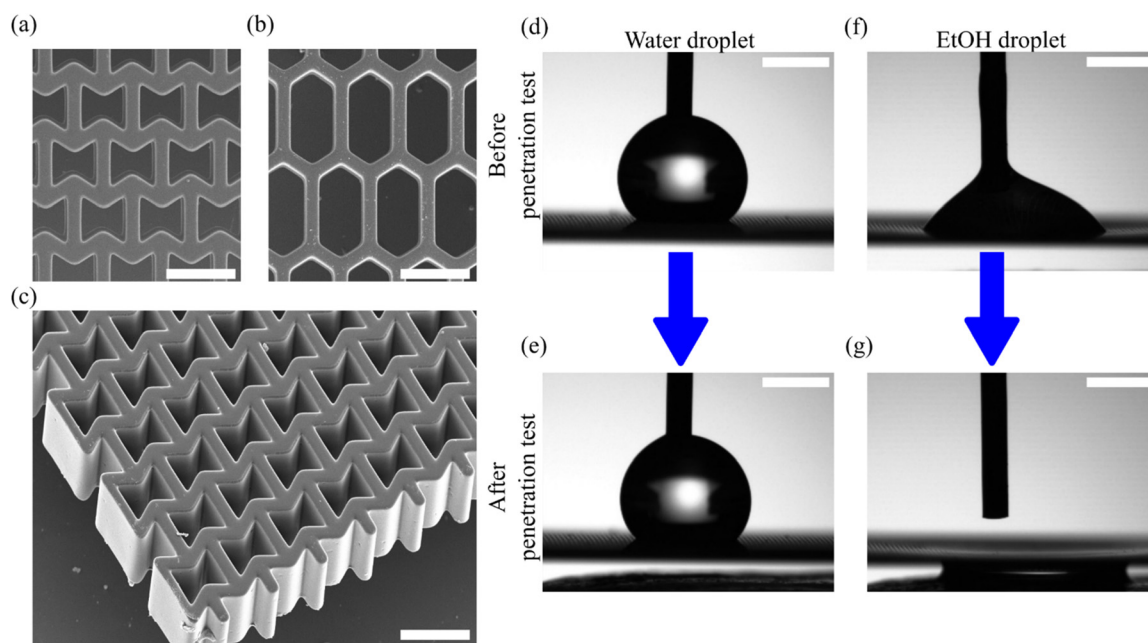


**FIG. 2.** SEM images of SU8 lattices (a) an auxetic structured bowtie lattice ( $\alpha = -30^\circ$ ), (b) a conventional honeycomb structured lattice ( $\alpha = +30^\circ$ ), and (c) an isometric view of the auxetic membrane after removal from the wafer showing membrane depth of  $125 \pm 5 \mu\text{m}$ . Drop penetration tests on an auxetic structured ( $\alpha = -30^\circ$ ) fluorosilanized SU8 surface, (d) water droplet before and (e) after touching underside of lattice. (f) EtOH droplet before and (g) after touching underside of lattice. All SEM images have a 100  $\mu\text{m}$  scalebar, and all drop penetration images have a 1 mm scalebar.



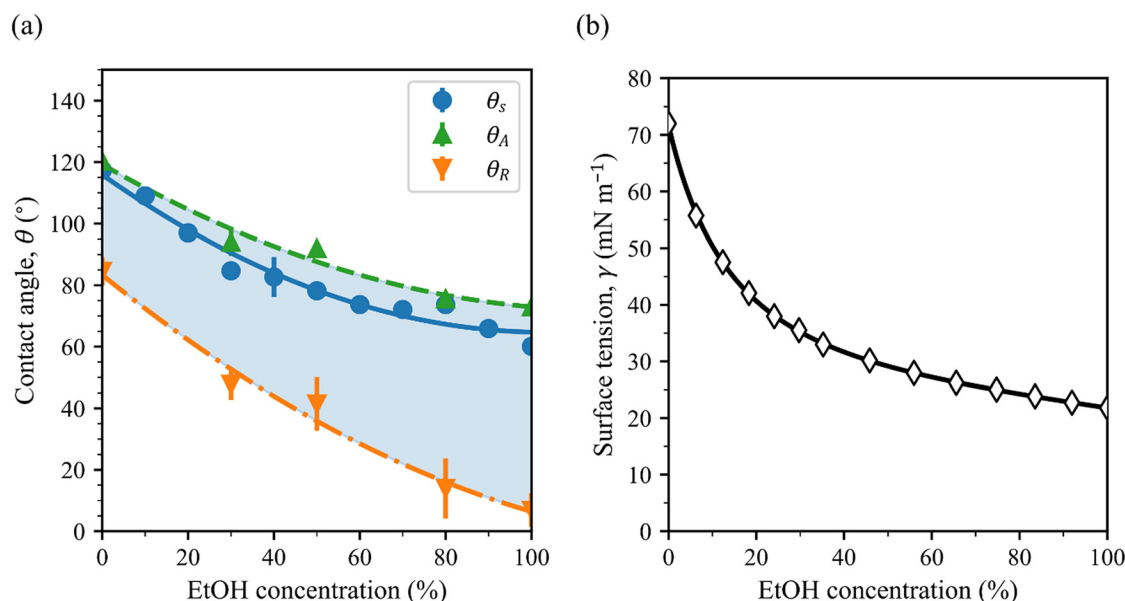


**FIG. 3.** (a) Contact angle as a function of EtOH concentration for Water/EtOH droplets on a solid flat fluorosilanized SU8 surface. Blue circles represent experimental data for static contact angles,  $\theta_s$ , green upward triangles represent experimental data for advancing contact angles,  $\theta_A$ , and orange downward triangles represent experimental data for receding contact angles,  $\theta_R$ . Each data set has a line representing the best second-degree polynomial fit. (b) Surface tension as a function of EtOH concentration. Reproduced with permission from Hamlett *et al.* Environ. Sci. Technol. **45**(22), 9666–9670 (2011). Copyright 2011 American Chemical Society.<sup>24</sup>

hysteresis are taken to describe the changing advancing and receding contact angles with increasing concentration (supplementary material). The pure EtOH receding contact angle appears to be almost completely pinned with,  $\Delta\theta_{CAH}(c = 100\%) = 66.2^\circ$ ,  $\theta_A(c = 100\%) = 73.0 \pm 2.1^\circ$ , and  $\theta_R(c = 100\%) = 6.8 \pm 5.5^\circ$ .

We next take a suspended fluorosilanized SU8 lattice with fixed auxetic rotation angle ( $\alpha = -30^\circ$ ) and look at how the static contact angle of the droplet changes with increasing EtOH concentration, while also testing whether the droplet is suspended or fully penetrated [Fig. 4(a)]. Second, the presence of the lattice decreases the solid–liquid

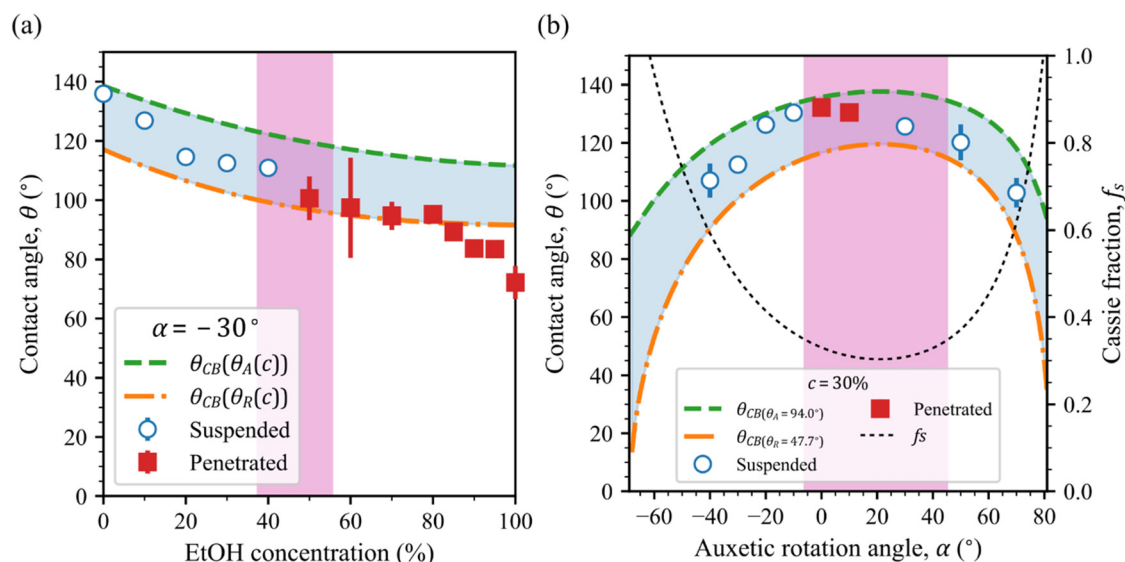


**FIG. 4.** (a) Contact angle as a function of EtOH concentration for water/EtOH droplets on an auxetic structured ( $\alpha = -30^\circ$ ) fluorosilanized SU8 surface. (b) Contact angle as a function of auxetic rotation angle on a fluorosilanized SU8 lattice for fixed state SU8 suspended models of ( $\alpha = -40^\circ$  to  $70^\circ$ ) at fixed 30% EtOH concentration. The vertical shaded region in both plots highlights the expected full-penetration from Eq. (6).

interface and has visibly increased the static contact angle of water from  $\theta_s(f_s = 1) = 117 \pm 1.7^\circ$  to  $\theta_s(f_s = 0.64) = 136.0 \pm 2.0^\circ$ , where  $f_s$  is the solid fraction of the auxetic geometry calculated using the analytical model developed by McHale *et al.* with the geometric parameters measured from SEM images of the lattice.<sup>10</sup> Penetration tests show that the droplets remain suspended up to concentrations of  $c = 40\%$ . From  $c = 50\%$  upward, the droplet always fully penetrates. It is observed that although the receding contact angle tends toward  $0^\circ$  for pure EtOH, the contact angles observed remains above  $60^\circ$  on the auxetic lattice. Next, we look at a fixed EtOH concentration ( $c = 30\%$ ) and change the auxetic rotation angle  $\alpha$  from  $-40^\circ$  to  $70^\circ$  [Fig. 4(b)]. For all auxetic rotation angles considered, the static contact angle for 30% EtOH/water mixture on the membrane [Fig. 4(b)] exceeds that for the flat fluorosilanized SU8 [ $\theta_s(c = 30\%) = 84.7 \pm 2.5^\circ$  with  $\Delta\theta_{CAH}(c = 30\%) = 46.3^\circ$ ,  $\theta_A(c = 30\%) = 94.0 \pm 4.5^\circ$  and  $\theta_R(c = 30\%) = 47.7 \pm 5.0^\circ$ —Fig. 3(a)]. The contact angles increase monotonically within the auxetic region ( $-40^\circ \leq \alpha < 0^\circ$ ), which follows expectations from our previous study.<sup>10</sup> Full-penetration occurs at the lowest solid fractions  $f_s = 0.33$  for  $\alpha = 0^\circ$  and  $f_s = 0.31$  for  $\alpha = 10^\circ$ . For the range  $30^\circ \leq \alpha \leq 70^\circ$ , the solid fraction increases and the droplets are once again suspended but now with a decreasing contact angle as the auxetic rotation angle increases.

We next look at the Cassie Baxter model for our case of a suspended membrane lattice. The simplified Cassie Baxter equation states the contact angle on a structured surface,  $\theta_{CB}$ , where liquid is bridging horizontally across flat topped pillars is given by

$$\cos \theta_{CB} = f_s \cos \theta_s - (1 - f_s), \quad (1)$$

where  $f_s$  is the fraction of the area under the droplet that is solid and  $\theta_s$  is the static contact angle on a smooth flat solid surface of the same chemical composition.<sup>16,25</sup> It is worth noting the static contact angle can lie anywhere between the bounds of the advancing or receding contact angle, i.e.,  $\theta_R \leq \theta_s \leq \theta_A$ . The solid fraction for the honeycomb lattice is defined by the rib parameters and the auxetic rotation angle. To directly compare the wetting response to the variation of the auxetic rotation angle, the ribs are assumed to be rotatable inextensible solid elements, as such we derive the solid fraction,  $f_s$ , as,

$$f_s(\alpha) = 1 - \frac{\left(l - \frac{t}{2 \cos \alpha}\right) \left[ \left(h - \frac{t(1 - \sin \alpha)}{\cos \alpha}\right) + \left(l - \frac{t}{2 \cos \alpha}\right) \sin \alpha \right]}{l(h + l \sin \alpha)}, \quad (2)$$

where  $h$  and  $l$  are the lengths of the horizontal and angled ribs, respectively [Figs. 1(a) and 1(b)],  $t$  is the rib thickness, and  $\alpha$  is the auxetic rotation angle [Fig. 1(d)]. A droplet will prefer to fully penetrate a structure over remaining suspended when,

$$\cos \theta_s < \cos \theta_{CM}, \quad (3)$$

where the critical contact angle is given by

$$\cos \theta_{CM} = -\frac{(1 - f_s)}{(r_W - 1)}. \quad (4)$$

where  $r_W$  is given in supplementary material. For a traditional superhydrophobic surface, the denominator in Eq. (4) would be  $(r_W - f_s)$ , but that is modified here in the membrane case to  $(r_W - 1)$ .<sup>15,17</sup>

When Eq. (3) is satisfied, from Eq. (4), a wetting transition on a membrane can only occur when

$$r_W > 2 - f_s. \quad (5)$$

We now test the model by looking at the agreement between the predicted angle from Eq. (1) and experiments. Figure 4(a) is in good agreement for the majority of concentrations,  $0\% \leq c \leq 80\%$ , between the upper and lower bounds of  $\theta_A$  (green dashed line) and  $\theta_R$  (orange dot-dash line) when using the concentration dependent advancing and receding contact angles from the fluorosilanized flat SU-8 surface in Eq. (1). The analytical model suggests that the minimum contact angle observed for pure EtOH is  $\theta_R = 91.6^\circ$  on the suspended auxetic lattice when inputting the receding contact angle for a smooth solid flat surface is  $\theta_R = 6.8^\circ$ . The change in contact angle with increasing concentration appears to follow Eq. (1) regardless of whether suspended or fully penetrated and does not appear to follow a Wenzel-type model (see supplementary material) in the latter case, which may be related to contact line pinning. However, experimentally, concentrations above 80% the contact angle appear to decrease below the expected predictions, which could be due to a secondary spreading regime, this is still much greater than the solid flat surface. The slight systematic decrease in the contact angles when fully penetrated between  $50\% \leq c \leq 80\%$ , could be attributed to a pinned contact line and a small loss of volume, which has wicked into the pores of the lattice. Calculating the change in contact angle through a loss of volume with a pinned contact line for the auxetic lattice predicts a change of  $\Delta\theta \sim 3.4^\circ$  (supplementary material). Another possible explanation could be that while care was taken to capture images of the droplets within a few seconds of touchdown onto the membrane, the decrease in angle could be due to a small amount EtOH evaporation for the highest concentrations, reducing the angle toward the receding angle. The analytic model also well describes the contact angle for the experiments in Fig. 4(b) for rotating auxetic rotation angle at fixed 30% EtOH concentration between the bounds of the advancing and receding contact angles.

We now look to see if the predictions of where the wetting transitions should occur agree with the experimental observations. We note that Eq. (5) predicts a fully suspended state or a fully penetrated only, it does not identify a partially penetrated state, although it is expected for chemically homogeneous and smooth vertical walls once a contact line begins to advance down the wall it will continue to a fully penetrated state.<sup>16</sup> In Fig. 4(a) for a fixed auxetic rotation angle,  $\alpha = -30^\circ$ , inputting the measured geometric parameters into Eqs. (2) and (S6) gives  $f_s = 0.49$  and  $r_W = 6.79$ , calculating the critical angle from Eq. (5),  $\theta_c = 84.9^\circ$ . Next, we find the concentration, which relates to the critical angle to determine the full-penetration concentration,  $c_p$ , if we use the advancing contact angle  $c_p(\theta_A) = 55\%$  and if we use the static contact angle  $c_p(\theta_s) = 37\%$ . Using the receding contact angle would yield full-penetration at every concentration. In Fig. 4(a), the vertical shaded region denotes the bounds between  $37\% \leq c_p \leq 55\%$ , which agrees with the experimentally observed full-penetration occurring between 40% and 50% EtOH concentration. In Fig. 4(b),  $f_s$  and  $r_W$  change as a function of the auxetic rotation angle. We first look at the advancing contact angle,  $\theta_A(c = 30\%) = 94 \pm 4.5^\circ$ ,  $\cos \theta_A = -0.07$ , which predicts full-penetration between  $-36^\circ \leq \alpha \leq 66^\circ$ . Both  $\theta_s = 84.7 \pm 2.5^\circ$  and  $\theta_R = 47.7 \pm 0.5^\circ$  predict that  $c = 30\%$  will always fully penetrate. The upper bound of the advancing contact angle,

$\theta_A = 98.5^\circ$ , predicts full-penetration between  $-6^\circ \leq \alpha \leq 45^\circ$ , shown in the vertical shaded region of Fig. 4(b), which appears to more reasonably agree with experiments. The lower bound of the advancing contact angle  $\theta_A = 89.5^\circ$  predicts the droplet will always fully penetrate. This suggests that the case for full-penetration is highly sensitive to small changes in the static contact angle on a flat surface  $\theta_s$ .

In conclusion, we experimentally observe the critical full-penetration angle of water/EtOH mixtures on superhydrophobic auxetic metamaterial membranes. We do this by developing a simple touch test to determine if a droplet is suspended on top of the lattice, or if it has fully penetrated, wicking through to the underside of the membrane. For an auxetic ( $\alpha = -30^\circ$ ) membrane we observe that the full-penetration occurs at 50% EtOH concentration, which relates to a  $\theta_s = 78.2 \pm 2.4^\circ$  on the solid flat surface and  $\gamma = 29.15 \text{ mN m}^{-1}$ . This compares favorably to theory which predicts full-penetration between  $37\% \leq c_p \leq 55\%$ . We also discuss the observed systematic decrease in contact angle for fully penetrated droplets, giving a possible attribution to a loss of volume into the membrane while the contact line is pinned. For a fixed EtOH concentration,  $c = 30\%$ , full-penetration is experimentally observed on auxetic rotation angles between  $0^\circ \leq \alpha \leq 10^\circ$ . This is within the bounds of the auxetic rotation angles for which full-penetration is predicted by theory,  $-6^\circ \leq \alpha \leq 45^\circ$ . This work helps to understand the relationship between surface tension, geometry and wetting transitions on superhydrophobic metamaterials, which is important for developing this new class of superhydrophobic materials.

See the supplementary material for video demonstrations for the touch test for suspended water and penetrated EtOH droplets; manufacture method of SU8 membranes; method of measurement of contact angles; polynomial fit of the advancing, receding, and static angles on flat fluorosilanized SU8; derivation of Wenzel-like contact angles; and penetrating state as a pinned base-volume loss mechanism.

The authors were supported in this work by funding from the UK Engineering & Physical Sciences Research Council (No. EP/T025158/1 and EP/T025190/1). M.M. was supported by the EPSRC CDT in Soft Matter for Formulation and Industrial Innovation, EP/S023631/1. For the purpose of open access, the author has applied a Creative Commons Attribution (CC BY) license to any Author Accepted Manuscript version arising from this submission.

## AUTHOR DECLARATIONS

### Conflict of Interest

The authors have no conflicts to disclose.

### Author Contributions

**Steven armstrong:** Conceptualization (lead); Data curation (lead); Formal analysis (lead); Investigation (lead); Methodology (equal); Project administration (supporting); Resources (equal); Software (lead); Validation (equal); Visualization (lead); Writing – original draft (lead); Writing – review & editing (lead). **Glen McHale:** Conceptualization (lead); Formal analysis (equal); Funding acquisition (lead); Methodology (equal); Project administration (lead); Supervision (lead); Validation (equal); Visualization (supporting); Writing – original draft (lead); Writing – review & editing (lead). **Andrew Alderson:** Conceptualization (lead); Formal analysis (equal);

Funding acquisition (lead); Methodology (equal); Project administration (lead); Supervision (lead); Validation (equal); Writing – original draft (equal); Writing – review & editing (equal). **Shruti Mandhani:** Conceptualization (supporting); Formal analysis (equal); Investigation (supporting); Methodology (equal); Software (supporting); Validation (equal); Writing – review & editing (equal). **Mahya Meyari:** Investigation (supporting); Methodology (supporting); Writing – review & editing (equal). **Gary George Wells:** Conceptualization (supporting); Funding acquisition (supporting); Methodology (equal); Project administration (supporting); Supervision (equal); Validation (equal); Writing – review & editing (equal). **Emma Carter:** Conceptualization (supporting); Formal analysis (supporting); Funding acquisition (supporting); Methodology (supporting); Supervision (equal); Writing – review & editing (equal). **Rodrigo Ledesma-Aguilar:** Conceptualization (supporting); Funding acquisition (supporting); Methodology (supporting); Supervision (equal); Writing – review & editing (equal). **Ciro Sempredon:** Conceptualization (supporting); Funding acquisition (supporting); Project administration (supporting); Supervision (equal); Writing – review & editing (equal).

## DATA AVAILABILITY

The data that support the findings of this study are available from the corresponding authors upon reasonable request.

## REFERENCES

- W. Barthlott and C. Neinhuis, "Purity of the sacred lotus, or escape from contamination in biological surfaces," *Planta* **202**(1), 1–8 (1997).
- C. Neinhuis and W. Barthlott, "Characterization and distribution of water-repellent, self-cleaning plant surfaces," *Ann. Bot.* **79**(6), 667–677 (1997).
- J. Zhang, J. Li, and Y. Han, "Superhydrophobic PTFE surfaces by extension," *Macromol. Rapid Commun.* **25**(11), 1105–1108 (2004).
- J. B. Pendry, "Negative refraction makes a perfect lens," *Phys. Rev. Lett.* **85**(18), 3966–3969 (2000).
- Z. G. Nicolaou and A. E. Motter, "Mechanical metamaterials with negative compressibility transitions," *Nat. Mater.* **11**(7), 608–613 (2012).
- M. Kadic, T. Bückmann, R. Schittny, and M. Wegener, "Metamaterials beyond electromagnetism," *Rep. Prog. Phys.* **76**(12), 126501 (2013).
- K. E. Evans, M. A. Nkansah, I. J. Hutchinson, and S. C. Rogers, "Molecular network design," *Nature* **353**(6340), 124 (1991).
- R. Lakes, "Foam structures with a negative poisson's ratio," *Science* **235**(4792), 1038–1040 (1987).
- R. S. Lakes, "Negative-Poisson's-ratio materials: Auxetic solids," *Annu. Rev. Mater. Res.* **47**, 63–81 (2017).
- G. McHale, A. Alderson, S. Armstrong, S. Mandhani, M. Meyari, G. G. Wells, E. Carter, R. Ledesma-Aguilar, C. Sempredon, and K. E. Evans, "Superhydrophobicity of auxetic metamaterials," *arXiv:2306.02916* (2023).
- T. Sun, L. Feng, X. Gao, and L. Jiang, "Bioinspired surfaces with special wettability," *Acc. Chem. Res.* **38**(8), 644–652 (2005).
- B. Bhushan and Y. C. Jung, "Natural and biomimetic artificial surfaces for superhydrophobicity, self-cleaning, low adhesion, and drag reduction," *Prog. Mater. Sci.* **56**(1), 1–108 (2011).
- J. Bico, U. Thiele, and D. Quéré, "Wetting of textured surfaces," *Colloids Surf., A* **206**(1–3), 41–46 (2002).
- J. Bico, C. Tordeux, and D. Quéré, "Rough wetting," *Europhys. Lett.* **55**(2), 214–220 (2001).
- D. Quéré, "Wetting and Roughness," *Annu. Rev. Mater. Res.* **38**(1), 71–99 (2008).
- N. J. Shirtcliffe, G. McHale, S. Atherton, and M. I. Newton, "An introduction to superhydrophobicity," *Adv. Colloid Interface Sci.* **161**(1–2), 124–138 (2010).
- D. Quéré, A. Lafuma, and J. Bico, "Slippery and sticky microtextured solids," *Nanotechnology* **14**(10), 1109–1112 (2003).



- <sup>18</sup>I. G. Masters and K. E. Evans, "Models for the elastic deformation of honeycombs," *Compos. Struct.* **35**(4), 403–422 (1996).
- <sup>19</sup>N. R. Geraldi, F. F. Ouali, R. H. Morris, G. McHale, and M. I. Newton, "Capillary origami and superhydrophobic membrane surfaces," *Appl. Phys. Lett.* **102**(21), 214104 (2013).
- <sup>20</sup>N. R. Geraldi, J. H. Guan, L. E. Dodd, P. Maiello, B. B. Xu, D. Wood, M. I. Newton, G. G. Wells, and G. McHale, "Double-sided slippery liquid-infused porous materials using conformable mesh," *Sci. Rep.* **9**(1), 13280 (2019).
- <sup>21</sup>P. M. King, "Comparison of methods for measuring severity of water repellence of sandy soils and assessment of some factors that affect its measurement," *Aust. J. Soil Res.* **19**(3), 275–285 (1981).
- <sup>22</sup>C. L. Watson and J. Letely, "Indices for characterizing soil-water repellency based upon contact angle-surface tension relationships," *Soil Sci. Soc. Am. J.* **34**(6), 841–844 (1970).
- <sup>23</sup>L. W. Dekker and C. J. Ritsema, "How water moves in a water repellent sandy soil: 1. Potential and actual water repellency," *Water Resour. Res.* **30**(9), 2507–2517, <https://doi.org/10.1029/94WR00749> (1994).
- <sup>24</sup>C. A. E. Hamlett, N. J. Shirtcliffe, G. McHale, S. Ahn, R. Bryant, S. H. Doerr, and M. I. Newton, "Effect of particle size on droplet infiltration into hydrophobic porous media as a model of water repellent soil," *Environ. Sci. Technol.* **45**(22), 9666–9670 (2011).
- <sup>25</sup>A. B. D. Cassie and S. Baxter, "Wettability of porous surfaces," *Trans. Faraday Soc.* **40**(0), 546 (1944).